STUDY OF THE NEUTRON COLLIMATOR DESIGN USED IN THE TAPIRO FACILITY FOR PATIENT TREATMENT WITH BNCT

Massimo Sarotto, Kenneth W. Burn, Lodovico Casalini, Elisabetta Nava, Carlo Petrovich

Italian Agency for new Technologies, Energy and Environment (ENEA), Via Martiri di Monte Sole 4, Bologna, Italy

ABSTRACT

In the Italian multidisciplinary BNCT (Boron Neutron Capture Therapy) project sponsored by MIUR, an analysis has been carried out to evaluate the possibility to irradiate patients with malignant brain gliomas at the ENEA TAPIRO 5 kW fast reactor (located at Casaccia, Rome). By means of an epithermal column mounted on one side of the core and a realistic anthropomorphic phantom placed at the column exit window in the side-of-cranium irradiation position, a series of Monte Carlo calculations with the MCNP (Monte Carlo N-Particle transport) code have shown the possibility to obtain a therapy beam able to fulfil all the BNCT requirements reaching treatment times lower than one hour.

This work is focused on the study of the column geometrical design that attempts to optimise the epithermal flux level, the beam quality and the collimation of the neutrons at the exit window where the head phantom is positioned. By means of an analogy with optics, it has been found that the best geometrical shape for the neutron collimator is the parabolic profile exploiting lead as the wall material. Even if in the first instance the parabolic choice seems to be an exotic solution, the Monte Carlo calculation results show excellent column performance and a good quality of all the reference free-beam parameters and in-phantom figures-of-merit used by the BNCT community. Since the parabolic shape could represent a problem in terms of feasibility of construction, some calculations employing plane geometry to fit the parabolic profile have been performed. A good compromise between the quality of the results and the technical feasibility has been obtained.

INTRODUCTION

In the NCT field, thermal-neutron research reactors are currently the most common source of neutron beams. To irradiate tumours located deeply in tissue, such as the glioblastoma multiform (GBM) brain tumours, an epithermal neutron beam becomes necessary. For this reason fast neutron reactors are also being considered as source. For both fast and thermal reactors, the fast neutrons coming from the core must be moderated by spectrum shifting or filtering techniques. Furthermore, a particular attention must be devoted to keeping the undesired neutron and gamma (γ) background dose within acceptable levels.

At ENEA, a study has been carried out in order to produce an epithermal neutron beam, suitable to irradiate patients affected by GBM brain tumours, by using the TAPIRO 5 kW fast reactor [1] as source. The reactor core is cylindrical and is made of 93.5% enriched uranium metal in a uranium-molybdenum alloy: it is totally surrounded by a copper reflector and a borate concrete shielding (about 170 cm thick). The outer part of the copper reflector and concrete biological shield have been removed from one azimuthal sector of the core to create a cavity (250 x 110 x 110 cm^3) for the epithermal column. The resulting window in the copper is currently filled with a thin layer of lead [2].

Since the irradiation position is outside the biological shield (at 262 cm from the core centre) and the reactor power is relatively low, careful design is necessary to achieve a sufficient neutron flux at the column exit window (only 25% of the suitable neutrons at the exit window come directly from the moderator zones, while the remaining 75% come from the reflection with the collimator walls).

This work is focused on the study of the column geometrical design that attempts to optimise the epithermal flux level, the beam quality and the collimation of the neutrons at the exit window where the head phantom is positioned. Of course the overall layout of the system and the choice of the materials to be used have been studied to fulfil all the BNCT requirements [3].

GEOMETRICAL DESIGN OF THE TAPIRO EPITHERMAL COLUMN

Fig. 1 shows the main geometrical variables describing the TAPIRO epithermal column. On the left part of Fig. 1 (where also a section of the irradiated phantom is schematised), the copper window, the AlF_3 (1.85 g/cm^3) moderator (l_{AlF3} = 31 cm) surrounded by a 7.5 cm thick nickel shield (light blue) and the lead collimator (grey) are shown. The nickel layer is relatively thin because its neutron reflection increases rapidly with the first few centimetres reaching quickly a plateau [4]. Furthermore, since the nickel produces γ radiation by (n, γ) reactions, its utilisation is limited to the beginning of the column (74.4 cm after the moderator [5]) to avoid γ shielding that will reduce the neutron fluence. The exit window (10 x 14 cm^2 [6]), where the head phantom is positioned, is preceded by a 7 cm nozzle and a 5 cm thick neutron absorber made of enriched lithiated polyethylene (blue) [7]. They have been added at the end of the column to increase the patient comfort and to provide an adequate protection to the rest of the body during head irradiation. Beyond the moderator, introduced to slow down the fast neutrons coming from the core and to obtain the desired spectrum, the column can be constructed varying: the reflector (l_{Refl}) and collimator (l_{Col}) lengths, and the shape of the collimator.

The extreme choices for the collimator geometry are (right part of Fig. 1):

1. The max. beam collimation / beam anisotropy (minimising the open cavity);
2. The max. open cavity radial dimensions.

The simulations performed show that, between these two extreme schemes (1), (2), the optimum compromise (first of all in terms of flux level at the exit window) is the parabolic shape (3) also schematised in Fig. 1. Since it could represent a problem in terms of feasibility of construction, some geometries exploiting linear planes to fit the parabolic profile can be utilised [4].

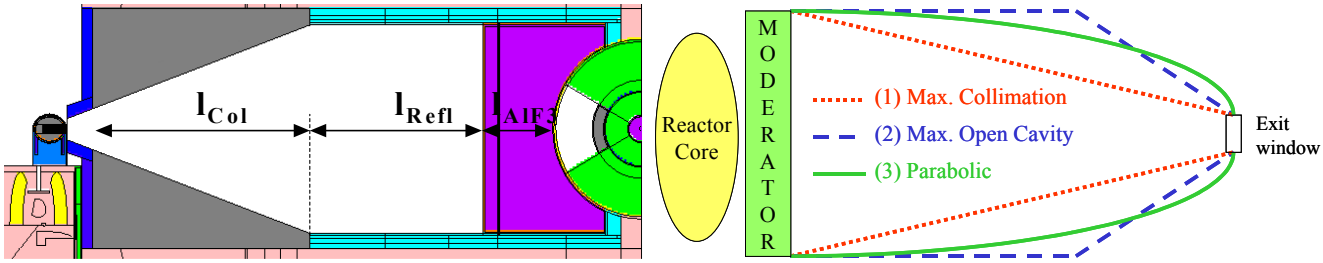

Fig. 1. Geometrical variables involved in the TAPIRO epithermal column design.

Another geometrical aspect to consider is that the column cavity has a square section and the desired exit window is rectangular (that covers better the cross section of the brain). Therefore the collimator parabolic profile has been obtained by means of four parabolic planes, instead of a paraboloid of revolution with a circular section.

CALCULATIONAL INSTRUMENTS

The MCNP code (ver. 4B) [8] has been employed with neutron cross sections from the ENDF/B-VI library [9]. To obtain an indication of the dose rates in human tissues, a realistic anthropomorphic phantom [10] has been placed at the column exit window in the side-of-cranium irradiation position. The S(α, β) model [11] has been used for thermal neutron scattering in biological tissue, considering also molecular and crystalline effects. Furthermore the DSA variance reduction optimiser, developed in-house (Direct Statistical Approach [12]), results particularly helpful to treat several responses simultaneously such as: the epithermal flux, the fast neutron and γ doses at the exit window or the dose components at various depths in phantom.

EXAMINED CONFIGURATIONS AND BEAM-IN-AIR PARAMETER RESULTS

This work is focused on two aspects of the column geometry (Fig. 1): the collimator shape and the relative lengths of the reflector (l_{Refl}) and collimator (l_{Col}) tracts. Varying these geometrical features, ten different column configurations have been examined by means of MCNP simulations. The final purpose is to obtain a high epithermal (0.4 eV < E < 10 keV) flux at the exit window, reducing fast and thermal neutrons and the energetic photons.

The geometrical characteristics of the examined schemes and the beam-in-air results (such as the neutron fluence, γ and fast neutron dose rates at the exit window), with their relative uncertainties at the 1σ level, are summarized in Table 1. The ten configurations are divided into three different classes depending on the relative lengths of the reflector and collimator. Configurations no. 1, 2, 3 belong to the first class representing the max. open cavity radial dimension geometry: the collimator is shaped by linear planes (no. 1), by four parabolic planes (no. 2) and by the fit of the parabolic profile by 2 linear planes (no. 3). Configurations no. 4, 5, 6 belong to the second class representing the max. collimation geometry: the collimator is shaped by linear planes (no. 4), by four parabolic planes (no. 5) and by the fit of the parabolic profile by 2 linear planes (no. 6). The third class represents a compromise between the previous two: the collimator is shaped by linear planes (no. 7), by parabolic planes (no. 8), and by the fit of the parabolic profile by 2 and 3 linear planes (respectively no. 9, 10). Fig. 2 shows the horizontal sections of some examined column geometries.

Conf. no.	Reflector l_{Refl} [cm]	Collimator l_{Col} [cm]	Geometric profile	$\Phi_{epith\ (0.4eV\text{-}10\ keV)}$ [n cm^{-2} s^{-1}]	J_{epith} / Φ_{epith}	$D_{fn\ (>10\ keV)}$ / Φ_{epith} [Gy cm^2]	D_{γ} / Φ_{epith} [Gy cm^2]
1	111.5	71.5	Linear	$7.026\cdot10^{8} \pm 0.002$	0.746 ± 0.003	$4.24\cdot10^{-13} \pm 0.006$	$4.04\cdot10^{-13} \pm 0.02$
2	111.5	71.5	Parabolic	$8.442\cdot10^{8} \pm 0.004$	0.676 ± 0.006	$4.12\cdot10^{-13} \pm 0.011$	$3.19\cdot10^{-13} \pm 0.03$
3	111.5	71.5	Parab. Fit	$7.287\cdot10^{8} \pm 0.003$	0.729 ± 0.003	$4.24\cdot10^{-13} \pm 0.007$	$3.80\cdot10^{-13} \pm 0.02$
4	46	137	Linear	$5.958\cdot10^{8} \pm 0.003$	0.796 ± 0.005	$4.24\cdot10^{-13} \pm 0.010$	$3.85\cdot10^{-13} \pm 0.03$
5	46	137	Parabolic	$8.588\cdot10^{8} \pm 0.008$	0.713 ± 0.011	$3.81\cdot10^{-13} \pm 0.022$	$2.51\cdot10^{-13} \pm 0.05$
6	46	137	Parab. Fit	$7.439\cdot10^{8} \pm 0.003$	0.757 ± 0.004	$4.15\cdot10^{-13} \pm 0.009$	$2.90\cdot10^{-13} \pm 0.02$
7	81.5	101.5	Linear	$6.619\cdot10^{8} \pm 0.003$	0.772 ± 0.005	$4.18\cdot10^{-13} \pm 0.010$	$4.54\cdot10^{-13} \pm 0.03$
8	81.5	101.5	Parabolic	$8.774\cdot10^{8} \pm 0.005$	0.693 ± 0.008	$3.92\cdot10^{-13} \pm 0.016$	$3.19\cdot10^{-13} \pm 0.04$
9	81.5	101.5	Parab. Fit	$7.421\cdot10^{8} \pm 0.003$	0.746 ± 0.005	$4.10\cdot10^{-13} \pm 0.010$	$3.83\cdot10^{-13} \pm 0.02$
10	81.5	101.5	Parab. Fit	$8.022\cdot10^{8} \pm 0.002$	0.728 ± 0.002	$4.08\cdot10^{-13} \pm 0.005$	$3.54\cdot10^{-13} \pm 0.01$

Table 1. Examined configurations and beam in-air-results at the collimator opening.

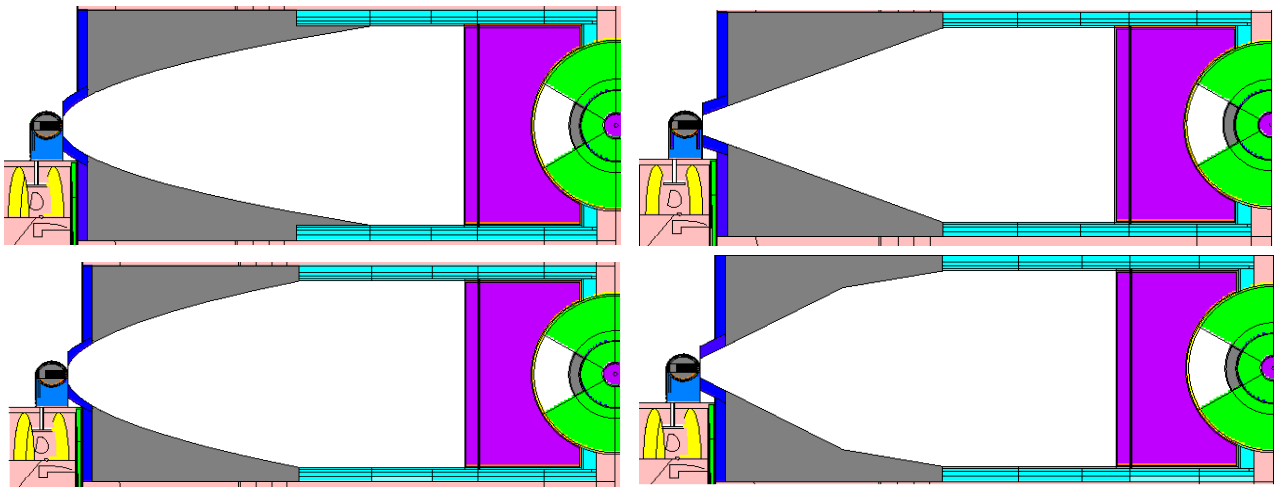

Fig. 2. Horizontal sections of some examined epithermal column configurations: no. 5, 7 (up); 8, 9 (down).

From Table 1 it is clear that:

- In each geometry class the collimator parabolic profile increases the epithermal flux level at the exit window by 20%, 44%, 30% (in the first, second, third class, respectively) in comparison with the linear collimator geometries. At the same time also the γ and fast neutron dose rates improve, while the beam collimation (J_{epith} / Φ_{epith}) results slightly worse.
- The parabolic fit by 2-3 linear planes also improves the epithermal flux level (in comparison with the linear geometries in the same class) but by a smaller amount: 4%, 23%, 12%, 21% in configuration no. 3, 6, 9, 10, respectively. While the γ and fast dose rates remain constant, the beam collimation results slightly worse, even if by a smaller amount than before.
- The higher flux at the exit window is obtained with configuration no. 8 (3rd class, parabolic).

IN-PHANTOM TREATMENT FIGURES-OF-MERIT RESULTS

The RBE (Relative Biological Effect), C-RBE (Compound Biological Effectiveness) factors and the ^{10}B concentrations in the different parts of the cranium utilised in the calculations are reported in Table 2 ([3], [13]). The compositions of the four different head regions (skin, tissue under skin, skull and brain) are defined as the ICRU 46 values for adult patients [14]. A mean high LET energy release of 2.34 MeV per $^{10}B(n,\alpha)^{7}Li$ reaction has been assumed [15].

Material	RBE for γ	RBE for n	^{10}B (μg / g)	^{10}B C-RBE factors
Skin	1	3.2	15	2.5
Tissue under skin	1	3.2	10	2.5
Skull	1	3.2	0	-
Healthy brain tissue	1	3.2	10	1.3
Tumour brain tissue	-	-	35	3.8

Table 2. The ^{10}B concentrations, RBE and C-RBE factors used in the calculations.

As shown in Table 3, an excellent quality of almost all in-phantom treatment figures-of-merit [3] is observed. The figures-of-merit calculated for each examined geometry are: the ADDR (max. dose rate to healthy tissue anywhere in the cranium), the AD and TD (depths in brain at which the tumour dose falls below a factor 2 and 1 of the max. healthy tissue dose, respectively), the treatment time (obtained imposing a max. healthy dose of 12.6 [Gy eq] and dividing this value by ADDR) and the PTR (the Therapeutic Ratio TR at a given depth is defined as the biological weighted dose to the tumour at that depth divided by the ADDR). All the dose values have been scored in small volume segments of dimensions (46 x 46 x 2) or (46 x 46 x 4) mm^3 around the head sagittal axis.

Config. no.	Advantage Depth Dose Rate [Gy eq min^{-1}]	Advantage Depth [mm]	Therapeutic Depth [mm]	Treatment Time [min]	Peak Therapeutic Ratio
1	0.2128 ± 0.005	71	51	59	4.205 ± 0.006
2	0.2484 ± 0.007	75	55	51	4.244 ± 0.008
3	0.2152 ± 0.004	73	52	59	4.234 ± 0.005
4	0.1894 ± 0.007	72	52	67	4.252 ± 0.008
5	0.2494 ± 0.013	75	53	51	4.302 ± 0.015
6	0.2202 ± 0.005	73	53	57	4.304 ± 0.007
7	0.2064 ± 0.007	72	51	61	4.208 ± 0.008
8	0.2525 ± 0.007	77	54	50	4.320 ± 0.010
9	0.2226 ± 0.006	72	52	57	4.252 ± 0.007
10	0.2348 ± 0.003	73	52	54	4.244 ± 0.004

Table 3. Treatment planning figures-of-merit results.

From Table 3 it results clear that, in each geometry class, the parabolic profile shortens the treatment time by about 15-25% and slightly improves the PTR values. The AD and TD seem to vary less but still show significant differences. Table 3 shows also that the second class (longest collimator) tends towards higher PTR values, while the third class tends towards shorter treatment times. The shortest treatment time (50 min) is obtained with configuration no. 8, presenting also the max. PTR value. Fig. 3 shows the dose profiles in brain for the column geometries of the third class. The advantages of the parabolic profile appear evident, both for the dose rate levels and for the TR values in brain tissue.

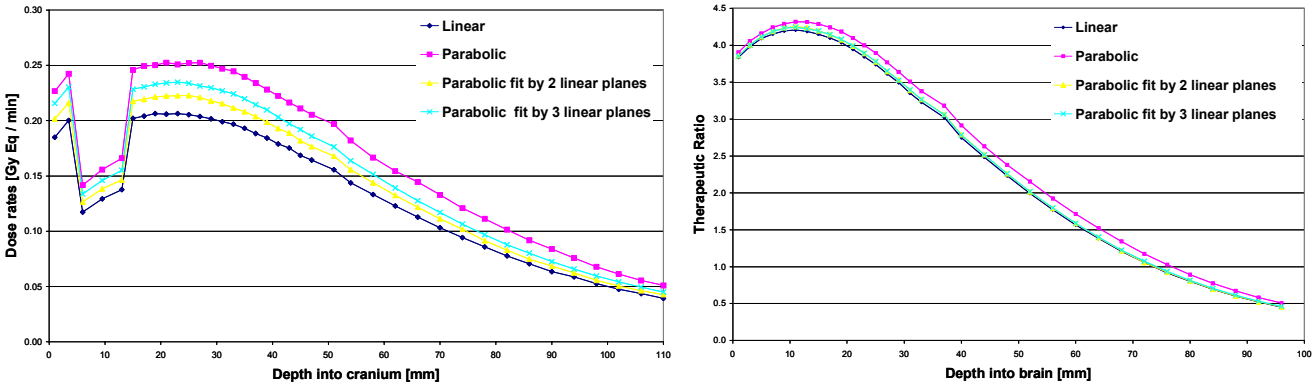

Fig. 3. Total dose rates in healthy tissues (left) and TR in brain (right) for configurations no. 7, 8, 9, 10.

ANALOGY WITH NON-IMAGING OPTICAL SYSTEMS

It is difficult to justify the advantages deriving from introduction of the parabolic column geometries. For this purpose, in the past some MCNP simulations were carried out to study the angular distribution of neutrons reflected by the column reflector/collimator walls. In particular it was confirmed that, starting from 10 keV energy neutrons impinging on a lead/nickel surface at various angles, the obtained reflected angular distributions are near-isotropic [4]. The direction of the emergent neutrons is of course a consequence of the multiple scattering events inside the examined material.

The nearly isotropic neutron reflection makes the geometry of the problem very similar to that of non-imaging optical systems [16]. These systems, whose main objective is to collect the maximum amount of light, represent the most efficient solution (better than that obtained by conventional image forming systems). The main characteristic of non-imaging systems is that, since the incoming radiation is neither collimated nor coming from a spatially limited source, image formation is not possible or, alternatively, it may not be convenient to collect light by an image system. The geometrical behaviour of the neutrons reflected from the lead or nickel layers is very similar to what happens in non-imaging systems. In fact, even if reflection by a generic optical system has always a mirror-like behaviour, to assume that a particle emerges from a surface in any direction (because the reflection is isotropic) is equivalent to assuming that the reflection is mirror-like with any direction of incidence (as for non-imaging systems). Among the different non-imaging optical systems, the parabolic shape is often the best solution: in this field it is called the Compound Parabolic Concentrator (CPC). A complete 3D CPC can be formed either by a paraboloid of revolution (circular section) or by extending two 2D parabola (four parabolic planes) forming a concentrator with a rectangular entrance and exit apertures (as in our case).

The best shape to maximise the neutron fluence at an exit window is the paraboloid of revolution with a circular section [4]. But since the TAPIRO column has a square section and it is preferable to work with rectangular exit windows, in this case the most suitable column profile is obtained by four parabolic planes. Even if the reasons given appear not to be rigorous but have, at least, an heuristic validity, the MCNP simulations carried out justify the chosen column shape.

CONCLUDING REMARKS

The TAPIRO epithermal column, currently under construction, contains some interesting features such as a thin nickel reflector, no thermal neutron or γ shield and an unconventionally shaped lead collimator. With the purpose to optimise the epithermal neutron flux at the exit window, this work analyses different geometries varying the relative lengths of the nickel reflector and lead collimator tracts, and the collimator shape. By means of Monte Carlo calculations, it has been found that a parabolic profile of the collimator gives the best column performances: projected therapy times for a single beam are around 50 minutes with a Peak Therapeutic Ratio value of 4.32.

Since the parabolic shape could represent a problem in terms of feasibility of construction, some calculations employing plane geometry to fit this profile have been performed. A good compromise between the column performances and the technical feasibility has been obtained.

REFERENCES

[1] K.W. Burn et al., Results of Monte Carlo neutronic calculations on the TAPIRO core for the reevaluation of the operating reactor power, Technical Report ENEA TLE TAPIRO 98/A - 005, December 1998.

[2] K.W. Burn et al., Design of an Epithermal Facility for treating Patients with Brain Gliomas at the TAPIRO Fast Reactor at ENEA Casaccia, Proc. X International Congress on NCT, Essen, Germany, September 2002.

[3] International Atomic Energy Agency, Current status of neutron capture therapy, IAEA-TECDOC-1223, Vienna, Austria, May 2001.

[4] M. Sarotto, A parabolic collimator as a possible solution in the TAPIRO epithermal column used for Patient Treatment with BNCT, Technical Report ENEA FIS P129 002, March 2003.

[5] G. Rosi et al., Role of the TAPIRO Fast Research Reactor in NCT in Italy. Calculations and Measurements, IAEA International Conference on Research Reactor Utilisation, Safety, Decommissioning, Fuel and Waste Management, Santiago, Chile, 10-14 November 2003.

[6] K. Skold, I Gudowska et al., The Swedish facility for boron neutron capture therapy, Proceedings of the IX International Symposium on Neutron Capture Therapy for Cancer, Osaka, 2000.

[7] L. Kankaanranta et al., First clinical results on the Finnish study on BPA-mediated BNCT in glioblastoma, Proceedings of the IX International Symposium on Neutron Capture Therapy for Cancer, Osaka, 2000.

[8] J.F. Briesmeister (ed.), MCNP^{TM} User's manual version 4B, LA-12625-M, LANL Report, 2000.

[9] Cross section Evaluation Working Group, ENDF/B-VI summary documentation, BNL-NCS-17541, National Nuclear Data Centre, Brookhaven National Laboratory, NY, 1991.

[10] R. Kramer et al., GSG-Bericht S-885 GSF - Forschungszentrum fur Umelt un Gesundheit, Neuherberg, Germany, 1982.

[11] J.T. Goorley, W.S. Kiger III, R.G. Zamenhof, Reference dosimetry calculations for neutron capture therapy with comparison of analytical and voxel models, Med. Phys., 29 (2), 2002.

[12] K.W. Burn et al., Variance Reduction with Multiple Responses, Proc. Conf. Monte Carlo 2000, Lisbon, Portugal.

[13] M.R. Palmer, R.G. Zamenhof et al., Treatment planning and dosimetry for the Harvard-Mit phase I clinical trial of cranial neutronic capture therapy, Int. J. Radiation Oncology Biol. Phys., Vol 53, no. 5, 2002.

[14] International Commission on Radiation Units and Measurements, Photon, Electron, Proton and Neutron Interaction data for body tissue, ICRU Report no. 46, 1992.

[15] D.A. Allen, T.D. Beynon, S. Green, Design for an accelerator-based orthogonal epithermal neutron beam for BNCT, Med. Phys. 26 (1), 1999.

[16] W. T. Welford, R. Winstom, The optics of nonimaging concentrators, Academic Press New York, NY, 1978.